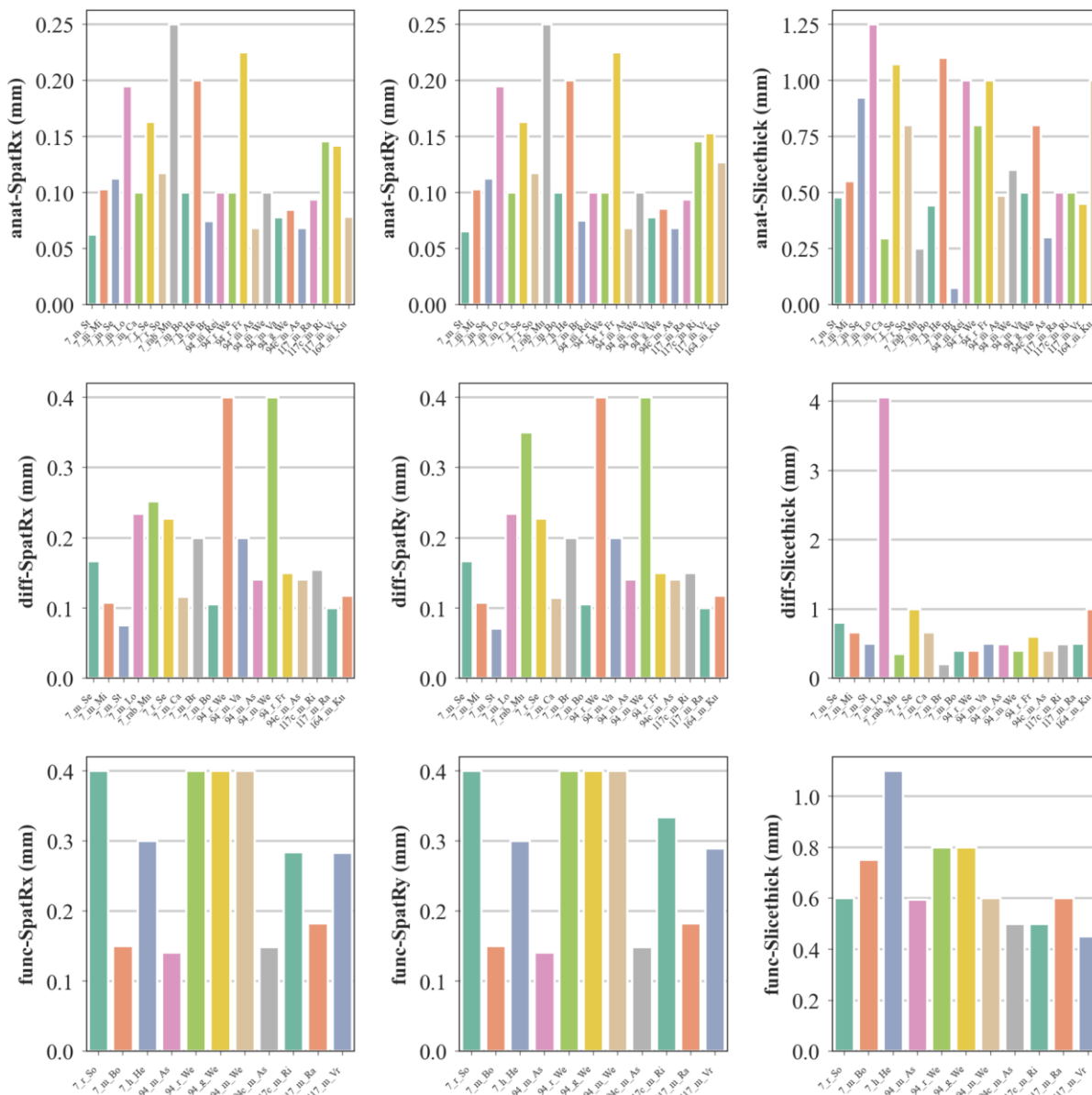
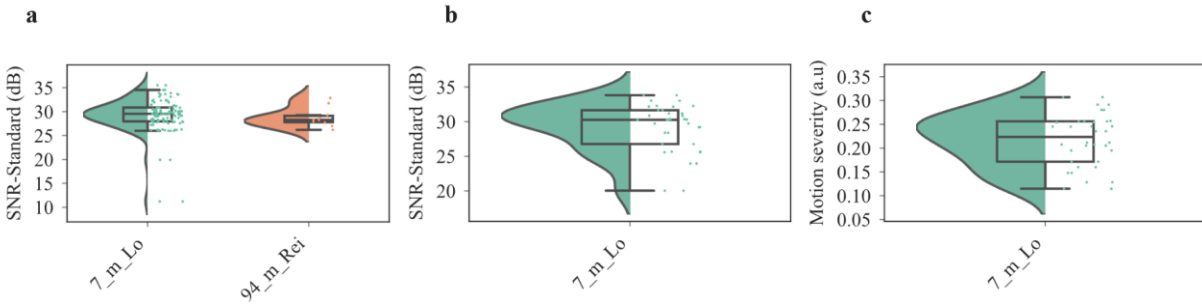


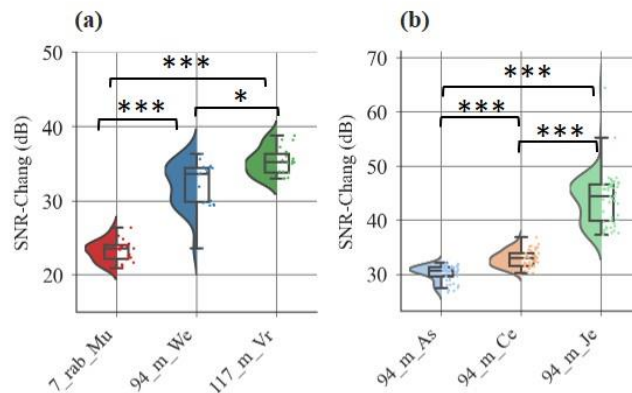
# SUPPLEMENTARY FIGURES AND TABLES



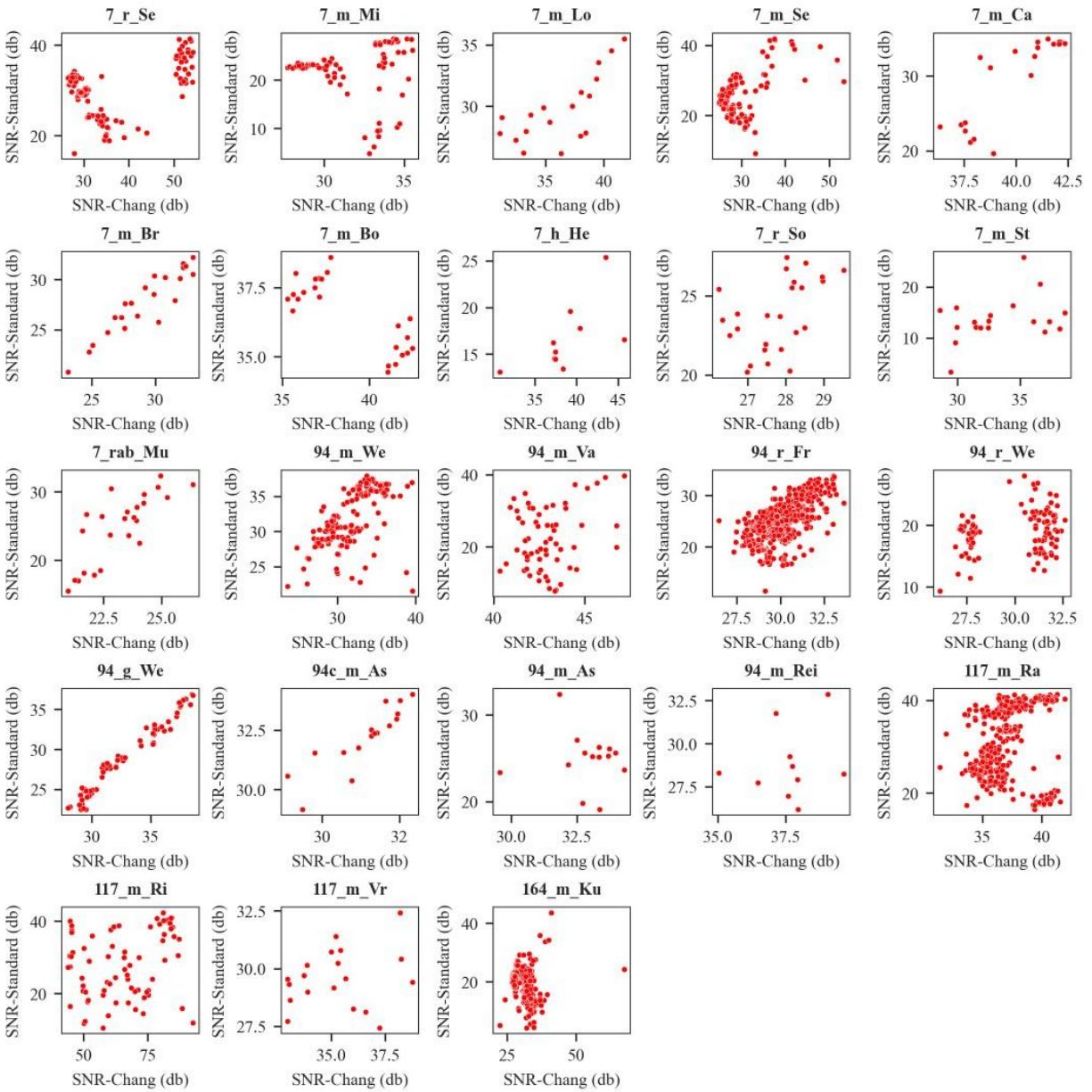
**Supplementary Figure 1: Summary of spatial resolution for all studies.** Spatial resolution in x- and y-direction (SpatRx, SpatRy) and slice thickness for all studies sorted into anatomical (anat), diffusion (diff), and functional (func) scans.



**Supplementary Figure 2: Summary of quality features for anatomical scans.** (a) SNR Standard for anatomical scans. (b) SNR Standard of diffusion scans. (c) Motion severity values for diffusion scans. This plot is the extension of Fig. 5 in the main manuscript for the two abdominal datasets 7\_m\_Lo and 94\_m\_Rei.



**Supplementary Figure 3: Comparison of the field strength and voxel size effect on SNR.** Significant differences were observed for SNR values (using the Chang method) between selected datasets with (a) different field strengths and (b) different voxel sizes. Voxel sizes: 7\_rab\_Mu (0.25x0.25x0.25 mm), 94\_m\_As (0.068x0.068x0.3 mm), 94\_m\_Ce (0.078x0.078x0.5), 94\_m\_Je (0.15x0.15x0.5), 94\_m\_We (0.1x0.1x0.4 mm), 117\_m\_Vr (0.142x0.153x0.45 mm). To determine significance, a Kruskal-Wallis test was initially conducted. Subsequently, a post hoc Dunn's multiple comparison test using the Holm–Bonferroni correction for p-value calculation was used. Significant differences between groups are shown as  $p < 0.05$  (\*),  $p < 0.01$  (\*\*),  $p < 0.001$  (\*\*\*)



**Supplementary Figure 4: Correlation of SNR-Standard and SNR-Chang for all anatomical datasets.**

## Role of the rating threshold for the agreement between manual raters and AIDAqc

In the following analysis, the predicted truth by manual raters was compared against the ratings generated by AIDAqc. Datasets with no true positive and/or false negative ( $TP+FN>0$ ) files were excluded to reduce the bias on the classification statistics, i.e., mitigate the impact of datasets where manual raters did not classify any files as “bad quality” (Table I). Further, different thresholds for the number of manual raters and AIDAqc outlier algorithms were compared.

The following metrics were used for a quantitative comparison:

1. Sensitivity: Out of all the actual “bad quality” datasets, how many were identified by AIDAqc as “bad quality” data?

$$Sensitivity = \frac{TP}{TP+FN}$$

2. Specificity: Out of all the “no bad quality” datasets, how many were identified by AIDAqc as such?

$$Specificity = \frac{TN}{TN + FP}$$

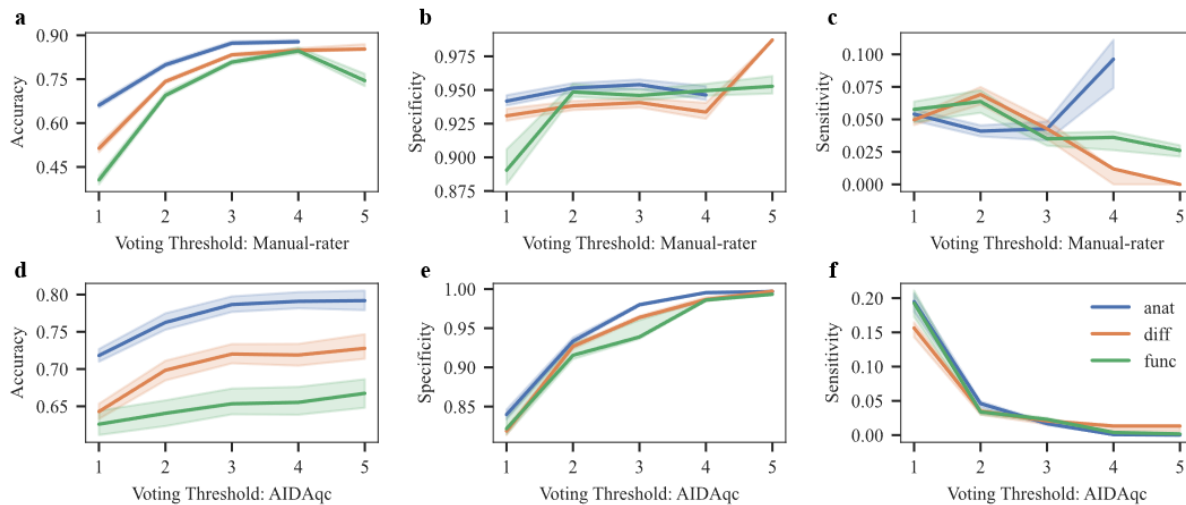
3. Accuracy: Out of all the classifications, what was the rate of correct classifications?

$$Accuracy = \frac{TP+TN}{TP+TN+FP+FN}$$

In the first comparison, the threshold for the manual voting was varied and the classification was statistically compared against all combinations of AIDAqc thresholds. The overall accuracy (rate of correct classifications) was relatively high across all manual rater voting thresholds for anatomical ( $0.77 \pm 0.21$ ), diffusion ( $0.70 \pm 0.25$ ), and functional ( $0.65 \pm 0.27$ ) scans (Supplementary Fig. 5a). The accuracy reached a maximum for anatomical and functional scans with the manual rater voting threshold set to four and for diffusion scans with the threshold set to five. For specificity, i.e., “how many true negatives” were identified by AIDAqc, the optimal manual votings threshold was four for anatomical ( $0.95 \pm 0.09$ ) and functional ( $0.93 \pm 0.15$ ) scans, respectively, and five for diffusion scans ( $0.94 \pm 0.08$ ) (Supplementary Fig. 5b). Sensitivity, a measure of how many true positive files were identified by AIDAqc, reached a peak with the manual rating

threshold of two for diffusion ( $0.05 \pm 0.13$ ) and functional ( $0.05 \pm 0.14$ ) scans, respectively, and for anatomical sequences with a threshold set to four ( $0.77 \pm 0.21$ ) (Supplementary Fig. 5c).

In the second comparison, the threshold for the AIDAqc voting was varied and the classification was statistically compared against all combinations of manual thresholds. Here, a consistent trend was observed: accuracy and specificity increased with the number of AIDAqc votes, whereas sensitivity reached the maximum already with the AIDAqc voting threshold set to one (Supplementary Fig. 5d-e). Average accuracy overall values for anatomical, diffusion, and functional scans were ( $0.77 \pm 0.21$ ), ( $0.70 \pm 0.25$ ), and ( $0.65 \pm 0.27$ ) respectively. For specificity, these values were ( $0.95 \pm 0.09$ ), ( $0.94 \pm 0.08$ ) and ( $0.93 \pm 0.15$ ). The highest sensitivity values for AIDAqc were reached with a threshold set to one for all sequence types. The average and std across all values for anatomical, diffusion, and functional were ( $0.05 \pm 0.14$ ), ( $0.05 \pm 0.13$ ), and ( $0.05 \pm 0.14$ ) respectively.



**Supplementary Figure 5: Statistical analysis of the classification.** Panels (a-c) showcase the dynamic interplay among accuracy, specificity, and sensitivity across varying manual rater voting thresholds. Panels (d-f) offer a parallel examination using AIDAqc voting thresholds. Each color represents a distinct sequence (anat - anatomical, diff - diffusion, and func - functional). The 30% confidence interval encapsulates the statistical uncertainty inherent in the plotted metrics. It is noteworthy that the condition  $(TP+TN)>0$  was applied before extracting these values; thus, some datasets ended up with no bad quality data when the manual-rater threshold was set to 5, as evident in the anatomical sequence in (a, c).

## Application of the outlier detection

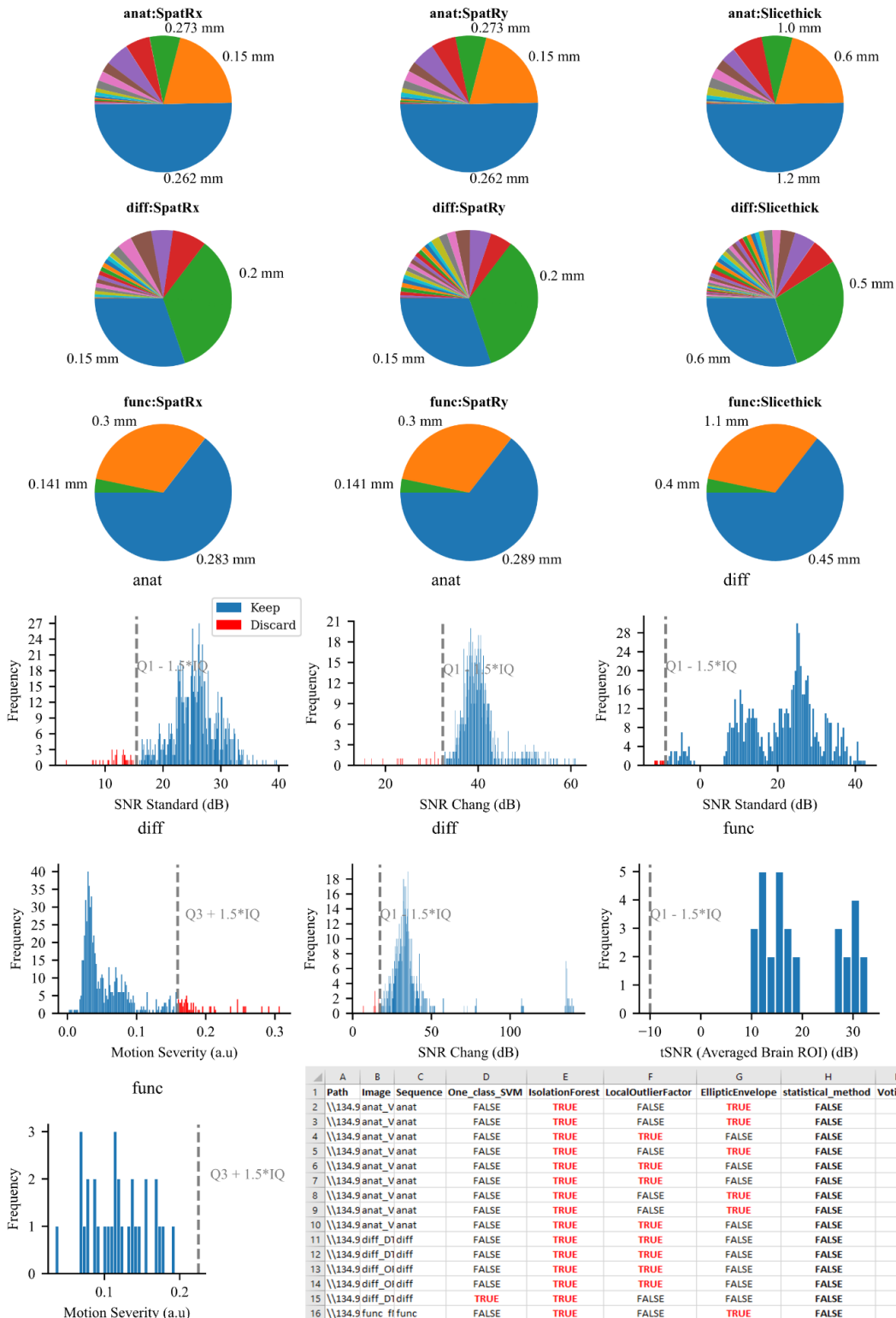
AIDAqc does not directly measure quantitative post-processing values. However, it is also important to note that the quality assessment based on factors like SNR or motion can indirectly affect processes such as brain extraction as shown in Supplementary Fig. 6, for the case with majority vote = 3. Problems in the subsequent processing steps can consequently lead to less precise quantitative values (Fig. 9).

[https://gin.g-node.org/Aswendt\\_Lab/2023\\_Kalantari\\_AIDAqc/src/master/output/SupplementFigures6.pdf](https://gin.g-node.org/Aswendt_Lab/2023_Kalantari_AIDAqc/src/master/output/SupplementFigures6.pdf)

**Supplementary Figure 6: Original DWI images and corresponding FA map pairs of all subjects from the dataset 94c\_m\_As and 94\_m\_As.** The majority vote for the image to be an outlier is written above each DWI image.

[https://gin.g-node.org/Aswendt\\_Lab/2023\\_Kalantari\\_AIDAqc/src/master/output/SupplementFigures7.pdf](https://gin.g-node.org/Aswendt_Lab/2023_Kalantari_AIDAqc/src/master/output/SupplementFigures7.pdf)

**Supplementary Figure 7: Overview of all subjects and extension of Fig. 10 in the manuscript.** For each subject, 4 different slices, and the registered atlas of those 4 different slices are shown. For the subject with the Majority Vote of 5, it can be seen that the brain extraction has completely failed along with the bias field correction, leading to a faulty atlas registration.



**Supplementary Figure 8: AIDAqc output statistics for all NifTI datasets** (Table I and Supplementary Table I). Pie diagrams show spatial resolution (in mm) for x, y, z direction. Bar plots show distribution of quality metrics. The table shows outliers not considered a statistical outlier but detected by the other algorithms.

BrkRaw GUI - v0.3.8-rc1

Open File | Open Directory | DataPath: 20220726\_092255\_A260722\_A260722\_1\_1 | Refresh

Account: nmr	Subject ID: A260722	DOB: 26 Jul 2022	Type: Quadruped
Scan Date: 2022-07-26, 09:22:55	Session ID: A260722	Sex: unknown	Position: Supine
Researcher: A260722	Study ID: 1	Weight: 0.001 kg	Entry: HeadFirst

Scan ID / Protocol | Slice Axis:  x  y  z

002::T2\_TurboRARE

003::T2\_TurboRARE

004::T2\_TurboRARE

005::T2\_weighted\_short\_Sth\_06

006::MPRAGE\_msP

007::LTS\_Multidelta2B\_Ageing

008::LTS\_Multidelta2B\_Ageing

009::LTS\_Charmed\_2B\_Ageing

010::B0Map-ADJ\_B0MAP

011::1\_Localizer

012::LTS\_Multidelta2B\_Ageing

013::LTS\_Multidelta2B\_Ageing

014::LTS\_Multidelta2B\_Ageing

015::LTS\_Multidelta2B\_Ageing

Selected Scan Info

Sequence: - Bruker:RARE **d**

Protocol: - T2\_TurboRARE

Scan Name: - T2\_TurboRARE (E2)

RepetitionTime: - 2500 msec

EchoTime: - 33 msec

FlipAngle: - 90 degree

PixelBandwidth: - 140.850 Hz

Dimension: - 2D

Matrix size: - 256 x 256 x 23

Number of SlicePacks: - 1

FOV size: - 35 x 35 (mm)

Spatial resolution: - 0.137 x 0.137 x 1.100 (mm)

---

Scan ID / Protocol | Slice Axis:  x  y  z

002::2a-RARE\_8\_coronal

003::2b-RARE\_8\_transverse

004::2c-RARE\_8\_sagittal

005::2c-RARE\_8\_sagittal

006::3-MSMEVTR-15122010

007::4-DWI\_2D\_15122010-150ms

Selected Scan Info

Sequence: - RARE (pvm) **f**

Protocol: - 2a-RARE\_8\_coronal

Scan Name: - 2a-RARE\_8\_coronal

RepetitionTime: - 1000 msec

EchoTime: - 23.334 msec

FlipAngle: - 180 degree

PixelBandwidth: - 195.312 Hz

Dimension: - 2D

Matrix size: - 256 x 256 x 8

Number of SlicePacks: - 1

FOV size: - 20 x 30 (mm)

Spatial resolution: - 0.125 x 0.125 x 1.000 (mm)

---

Scan ID / Protocol | Slice Axis:  x  y  z

001::01\_Localizer

002::02\_Localizer\_multi\_slice

003::03\_T2\_FLASH\_axial

004::04\_T2\_FLASH\_coronal

005::06\_fmri\_single

006::B0Map-ADJ\_B0MAP

007::07\_fmri\_multi\_trigger

008::08\_DTI\_EPI\_36dir

009::09\_MRS\_water\_pfc

010::09\_MRS\_water\_pfc

012::09\_MRS\_water\_pfc

013::09\_MRS\_water\_pfc

014::09\_MRS\_water\_pfc

015::10\_MRS\_meta\_pfc

016::11\_MRS\_water\_thal

017::11\_MRS\_water\_thal

018::20\_MRS\_meta\_thal

019::09\_MRS\_water\_pfc

020::09\_MRS\_water\_pfc

021::20\_MRS\_meta\_thal

Selected Scan Info

Sequence: - Bruker:FLASH **h**

Protocol: - 03\_T2\_FLASH\_axial

Scan Name: - 03\_T2\_FLASH\_axial (E3)

RepetitionTime: - 200 msec

EchoTime: - 3.1 msec

FlipAngle: - 25 degree

PixelBandwidth: - 822.368 Hz

Dimension: - 2D

Matrix size: - 120 x 100 x 20

Number of SlicePacks: - 1

FOV size: - 17 x 15 (mm)

Spatial resolution: - 0.142 x 0.150 x 0.500 (mm)

Temporal resolution: - 45600.000 (msec)

Reco ID / DataType | Slice: 10

001::MAGNITUDE IMAGE



**Supplementary Figure 9: Orientatiion in datasets.** Three exemplary subjects from three different datasets from Table I. Multiple TurboRARE sequences with the same sequence, protocol, and scan names (d) but scanned with different orientations (a), (b), wherein the second subject, this was mentioned in the protocol and scan name (f). Subject alignment is supine in (c) whereas in (e) it is set as supine but right to left. In the third subject, both subject alignment and orientation were done in a standard norm (g,h). AIDAqc's current limitation lies in comparing different orientations such as (a), (b), and (c), which may raise questions. It might not lead to outliers if the cohort of subjects has the same sequences, but it still may be questionable and would require further automatic adjustment in terms of how the algorithm extracts the SNR, motion, and ghosting.

**Supplementary Table I: Summary of datasets used for developing AIDAqc**

	Repository	Datasets	Species	Scanner (Vendor, field strength/bore size, electronics, gradient, Tx/Rx coils)	Modalities	Sequences	Data format	Sample size (n)
1	Aswendt	94_m_As	Mouse brain	Bruker Biospec 94/20 with AVANCE II electronics. Gradient: B-GA12SHP (660 mT/m and slew rates up to 4570 T/m/s). TX/RX: 1H quadrature cryogenic surface coil or 1H mouse brain quadrature surface.	T2w, rs-fMRI, DTI	TurboRARE, GE-EPI, SE-EPI	Bruker raw	32
2	Aswendt	94c_m_As	Mouse brain	Bruker Biospec 94/20 with AVANCE II electronics. Gradient: B-GA12SHP (660 mT/m and slew rates up to 4570 T/m/s). TX/RX: 1H quadrature cryogenic surface coil or 1H mouse brain quadrature surface.	T2w, rs-fMRI, DTI	TurboRARE, EPI, DTI, BIS, GRE, FMRI	Bruker raw	32
3	Boehm-Sturm	7_m_Bo	Mouse brain	Bruker Biospec 70/20USR with AVANCE III HD electronics. Gradient: BGA-12S HP (440 mt/m and slew rates up to 3440 T/m/s). TX/RX: 1H quadrature cryogenic surface coil	T2w, DTI	TurboRARE, DTI, EPI, SEG, T2STAR	Bruker raw	27
4	Carnevale	7_m_Ca	Mouse brain	Bruker Pharmascan 70/16US mm with AVANCE III HD electronics. Gradient: BGA9SHP, Tx: 1H RF circularly polarized 72 mm volume coil. RX: 1H mouse brain quadrature surface.	3D-T2/DTI	TurboRARE, DTI, EPI	Bruker raw	20
5	Franx	94_r_Fr	Rat brain	Varian/Agilent 94/210 mm bore. Gradient: 205_120_HD gradient (400 mT/m), Tx: 80 mm Helmholtz coil, Rx: 15 mm inductively coupled surface coil receive	T2w, DWI, T1w	multishot EPI spin-echo, 2D gradient echo	Nifti	722
6	Hekmatyar	7_h_He	Hamster brain	Bruker Biospec 70/20. Gradient: NA. 2x2 1H Rat brain surface array coil 400 mT/mm 12 cm inner diameter)	T2w, rs-fMRI	2D Single shot spin echo EPI (SE-EPI)	Nifti	10
7	Kurniawan	164_m_Ku	Mouse brain	Bruker Biospec 164/89 vertical. Gradient: micro 2.5 gradient max 1.5T/m using Great 60 gradient amplifier. Avance II electronics. Tx/Rx: SAW 20 mm mouse head coil.	T2w, DTI	RARE, DWI	Bruker raw	168
8	Micotti	7_m_Mi	Mouse brain	Bruker Biospec 70/30 with AVANCE III electronics. Gradient: BGA12SL gradient (440 mT/m and slew rates up to 3440 T/m/s). Tx: 1H RF circularly polarized 72 mm volume coil. RX: 1H mouse brain quadrature surface.	T2w, DTI	RARE_PO, SIZ_AXIAL, DTI_RETE	Bruker raw	21
9	Muñoz-Moreno	7_rab_Mu	Rabbit brain <sup>1</sup>	Bruker Biospec 70/30 with AVANCE III electronics. Gradient: BGA12S (400 mT/m, 12 cm inner diameter) . Tx: NA. Rx: NA.	T1w, DWI	7T T1w (MDEFT), DWI	Nifti	24
10	Brinton	7_m_Br	Mouse brain	Bruker Biospec 70/20 and Bruker 300 1H 2x2 mouse brain surface array or 300 1H 2x2 rat brain surface array	T2w, DWI	TurboRARE, 3D DTI, EPI	Nifti	20

11	Ramos-Cabrer	117_m_Ra	Mouse brain	Bruker Biospec USR 117/16 with AVANCe III electronics. Gradient: BGA-9S (750 mT/m strength, and 6600 T/m/s slew rate). Tx: Bruker's 500 1H RF circularly polarized 72 mm volume coil, RX: Bruker's RF 500 1H – Mouse Brain SUC surface coil OR Neos Biotech's mouse brain surface coil.	T2w, DTI, rs-fMRI	TurboRARE, FLASH, EPI	Bruker raw	69
12	Reichardt	94_m_Rei	Mouse abdominal	Bruker Biospec 94/20 mm with Avance3 electronics. Gradient: B-GA 12S., 680 mT/m, Tx/RX .1H mouse quadrature volume coil (38mm ID)	T2w	T2_TRARE	Bruker raw	10
13	Rivera-Olvera	117_m_Ri	Mouse brain	Bruker Biospec USR 117/16, B-GA9S (600 mT/m and slew rates up to 6000 T/m/s) ; TX/RX: 1H quadrature cryogenic surface coil.	T2w, DTI, rs-fMRI	DTIEPI, FLASH, EPI	Bruker raw	20
14	Sta Maria	7_m_St	Mouse brain	7T PET-MR system (MR Solutions Ltd, Guildford, UK), bore size: ~ 24 cm, gradient strength: 600 mT/m, coil: 20 mm inner diameter, 18 mm length, quadrature birdcage	T2w, DTI	FSE, FLASH, SE-EPI	Nifti	17
15	Selim	7_m_Se	Mouse/rat brain	Bruker Biospec 70/30, Bruker 300 1H 2x2 mouse brain surface array or 300 1H 2x2 rat brain surface array	T2w/T1w/DTI	TurboRARE, WEIGHTED_SHORT, SDS	Bruker raw	20/30
16	Selim	7_r_Se	Mouse/rat brain	Bruker Biospec 70/30, Bruker 300 1H 2x2 mouse brain surface array or 300 1H 2x2 rat brain surface array	T2w/T1w/DTI	TurboRARE, LTS, T2_WEIGHTED_SHORT	Bruker raw	20/30
17	Soria	7_r_So	Rat brain	7T Bruker Biospec 70/30 horizontal animal scanner (400 mT/m, 12 cm inner diameter), 1H 2x2 rat brain surface array	T2w, rs-fMRI	7T T2w (RARE),rs-fMRI	Nifti	8 (multiple time points)
18	Van Leeuwen	94_m_Va	In vivo mouse brain	9.4 T Varian/Agilent, quadrature birdcage with ID 35 mm, 115_60_HD gradient (1000 mT/m)	T2w, DTI	TurboRARE	Nifti	131
19	Vrooman	117_m_Vr	In vivo mouse brain	Bruker Biospec USR 117/16, B-GA9S (600 mT/m and slew rates up to 6000 T/m/s) ; Mouse with single loop 10 mm diameter Rx surface coil and 089/072 mm Tx volume resonator.	T2w, GE-EPI	TurboRARE /rs-fMRI	Nifti	12 (multiple time points)
20	Wenk	94_m_We	In vivo mouse/rat/gerbil brain	9.4 Bruker Biospec USR 94/20, B-GA12SHP (660 mT/m and slew rates up to 4570 T/m/s) ; Mouse with Array coil + 112/086 volume resonator; Gerbil with single-loop coil ID15 + 112/086 volume resonator; Rat with 075/40 volume resonator	T2w, rs-fMRI, fMRI, DTI	T2_ANATOMY, DTI_EPI_ISO, T2STAR, AUDISTIM	Bruker raw	46/32/25
21	Wenk/Goncalves	94_r_We	In vivo mouse/rat/gerbil brain	9.4 Bruker Biospec USR 94/20, B-GA12SHP (660 mT/m and slew rates up to 4570 T/m/s) ; Mouse with Array coil + 112/086 volume resonator; Gerbil with single-loop coil ID15 + 112/086 volume resonator; Rat with 075/40 volume resonator	T2w, rs-fMRI, fMRI, DTI	T2_ANATOMY, DTI_EPI_ISO, RSFMRI_EXPERIMENT	Bruker raw	46/32/25

22	Wenk/Michael	94_g_We	In vivo mouse/rat/gerbil brain	9.4 Bruker Biospec USR 94/20, BGA12SHP (660 mT/m and slew rates up to 4570 T/m/s) ; Mouse with Array coil + 112/086 volume resonator; Gerbil with single-loop coil ID15 + 112/086 volume resonator; Rat with 075/40 volume resonator	T2w, rs-fMRI, fMRI, DTI	T2_TURBO RARE, NON_ROTATING_EPI	Bruker raw	46/32/25
23	Longo	7_m_Lo	In vivo mouse abdominal	7T MicroImaging Bruker Avance III, 1H 30mm TX/RX body volume coil	T2w, DTI	T2 mic_rare, DtiEpi	Bruker raw	20

<sup>1</sup>ex vivo. Abbreviations: DTI (Diffusion Tensor Imaging), NA (details not available), rs-fMRI (resting-state functional MRI), T2w (T2-weighted MRI), Tx (transmit coil), Rx (Receive coil)

**Supplementary Table II:** Summary of published datasets used for testing AIDAqc

	Repository	Species /Target	Scanner	Sequences	Data types	Ref.
1	Aswendt	Mouse	9.4T Bruker, cryocoil	T2-weighted, rs-fMRI	Bruker raw	[63] <a href="https://doi.org/10.17617/3.5p">https://doi.org/10.17617/3.5p</a>
2	Jelescu	Rat	14T Varian System	T2-weighted, DTI, rs-fMRI	Nifti	<a href="https://openneuro.org/datasets/ds003520/versions/1.0.2">https://openneuro.org/datasets/ds003520/versions/1.0.2</a> <a href="https://openneuro.org/datasets/ds004441/versions/1.0.1">https://openneuro.org/datasets/ds004441/versions/1.0.1</a>

**Supplementary Table III:** Confusion matrix visualizing the statistical definition used to classify the data.

<i>Total</i>	<i>AIDAqc predicted positive (bad quality data)</i>	<i>AIDAqc predicted positive (no bad quality data)</i>
<i>Manual rater assigned positive (bad quality data)</i>	True positive (TP)	False negative (FN)
<i>Manual rater assigned negative (no bad quality data)</i>	False positive (FP)	True negative (TN)